



## Utilization of a 3D-printed model for preoperative planning and operative osteotomy of a pediatric cubitus varus deformity



Karen M. Bovid, MD <sup>a,\*</sup>, Evan J. Kohler, BS <sup>a</sup>, Jason M. Habeck, MD <sup>b</sup>,  
Peter A. Gustafson, PhD <sup>c</sup>

<sup>a</sup> Department of Orthopaedic Surgery, Western Michigan University Homer Stryker M.D. School of Medicine, Kalamazoo, MI, USA

<sup>b</sup> Watertown Regional Medical Center, Watertown, WI, USA

<sup>c</sup> Department of Mechanical and Aerospace Engineering, Western Michigan University, Kalamazoo, MI, USA

Cubitus varus is a challenging-to-treat complication following pediatric fractures of the elbow.<sup>2</sup> This is typically thought to occur secondary to malunion of the fracture or uneven growth resulting in varus angulation.<sup>9,10</sup> “Classic” cubitus varus deformity typically consists of varus, extension, and internal rotation, with varying degrees of deformity in any of those planes.<sup>18</sup> The multiplanar nature of this deformity frequently causes cosmetic issues and occasionally compromises function or results in a tardy ulnar nerve palsy.<sup>9</sup> Several types of corrective osteotomies have been described in the literature.<sup>1,4,6,7,11,12,14,16,19,22</sup> Axial imaging, typically with computed tomography, has been used to aid in preoperative planning.<sup>6,13,18,20,21,23,24</sup> However, computed tomography has many limitations compared to magnetic resonance imaging (MRI), especially with regard to the visualization of cartilage and other nonossified tissues in the skeleton of pediatric patients. With the development and increasing prevalence of 3-dimensional (3D) printing, this modality has great advantages for use in planning deformity correction.<sup>1,6,7,11,12,14,16,19,22</sup> This study describes the use of MRI with 3D modeling and printing for the preoperative planning and operative execution of a supracondylar humerus osteotomy for correction of cubitus varus.

### Case report

A 3-year-old right hand–dominant boy with no significant past medical history was seen in the Pediatric Orthopedic Surgery clinic with complaints of right elbow deformity that developed after nonoperative treatment of a right humerus lateral condyle fracture sustained 2 years prior. The patient reported intermittent pain and

used his left hand for most activities during the day. He had met all other developmental milestones for his age and had otherwise been healthy. On physical examination, the patient's right arm had a cubitus varus deformity with a lateral bony prominence (Fig. 1). Carrying angle was 18° of varus on the right upper extremity and 5° of valgus on the left. He had mildly decreased flexion on the right compared to the left, but otherwise had full range of motion. His neurovascular examination was normal. Plain radiographs confirmed a cubitus varus angulation with internal rotation of the capitellum and a bony prominence at the lateral epicondyle (Fig. 2, A and B). Humerus–elbow–wrist angle was 29° of varus on the right and 10° of valgus on the left. The angle between the humeral epicondyles and humeral shaft was 71° of varus on the right and 90° on the left. Tilt angle was 29° on the right and 24° on the left.

The family requested surgical correction of the right elbow deformity, and a right lateral closing wedge supracondylar



**Figure 1** Clinical photograph of the patient's right arm demonstrating cubitus varus deformity with varus carrying angle and internal rotation of the distal humerus.

The Western Michigan University Homer Stryker M.D. School of Medicine Institutional Review Board has determined case reports to be exempt from review. The patient's parents consented to publication of this case report.

\* Corresponding author: Karen M. Bovid, MD, 1000 Oakland Drive, Kalamazoo, MI 49008.

E-mail address: [karen.bovid@med.wmich.edu](mailto:karen.bovid@med.wmich.edu) (K.M. Bovid).

<https://doi.org/10.1016/j.jses.2019.05.003>

2468–6026/© 2019 The Authors. Published by Elsevier Inc. on behalf of American Shoulder and Elbow Surgeons. This is an open access article under the CC BY-NC-ND license (<http://creativecommons.org/licenses/by-nc-nd/4.0/>).

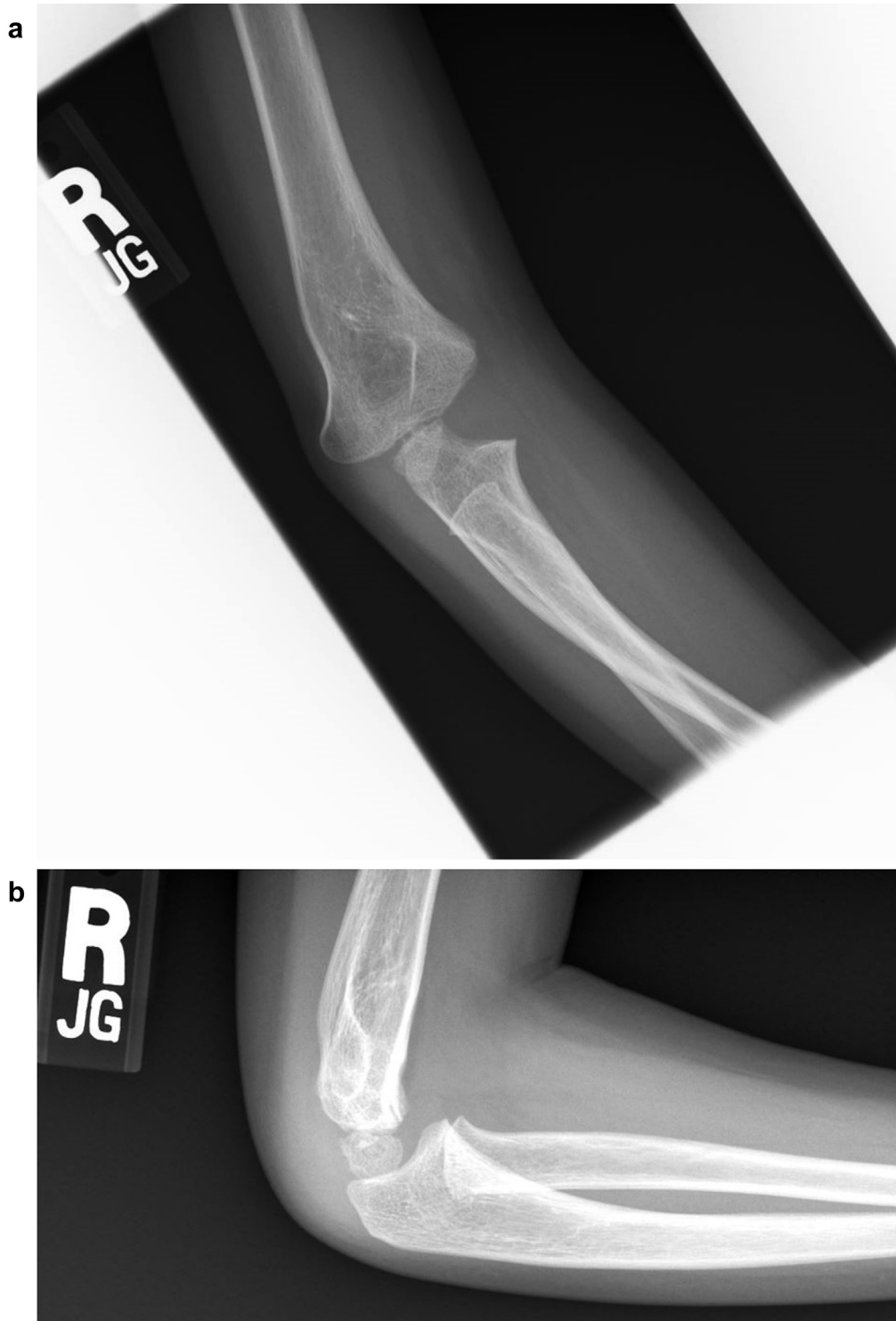


**Figure 2** Anteroposterior (a) and lateral (b) radiographs of the right elbow demonstrating cubitus varus deformity.

humerus osteotomy with right elbow arthrogram was recommended. During preoperative planning, MRI of the right elbow without contrast was obtained for better visualization of the deformity, including the cartilaginous portions of the epiphysis and alignment of the articular surfaces. Segmentation was completed using 3D Slicer (version 4.5, <https://www.slicer.org/>, accessed August 2018) to convert the images to a 3D surface representation of the bony/cartilaginous anatomy of the distal humerus (Figs. 3

and 4). The surfaces were used to 3D-print physical representations of the deformity. Corrective osteotomy was planned using Boolean operations and surface transformations (ie, virtual corrective osteotomy) on the computer model (Fig. 5) using FreeCAD (version 0.16, <https://www.freecadweb.org/>, accessed September 2018). Subsequently, 2 simulated physical corrections were performed in the lab using 3D-printed models (Fig. 6). This allowed formulation of a precise operative osteotomy plan.

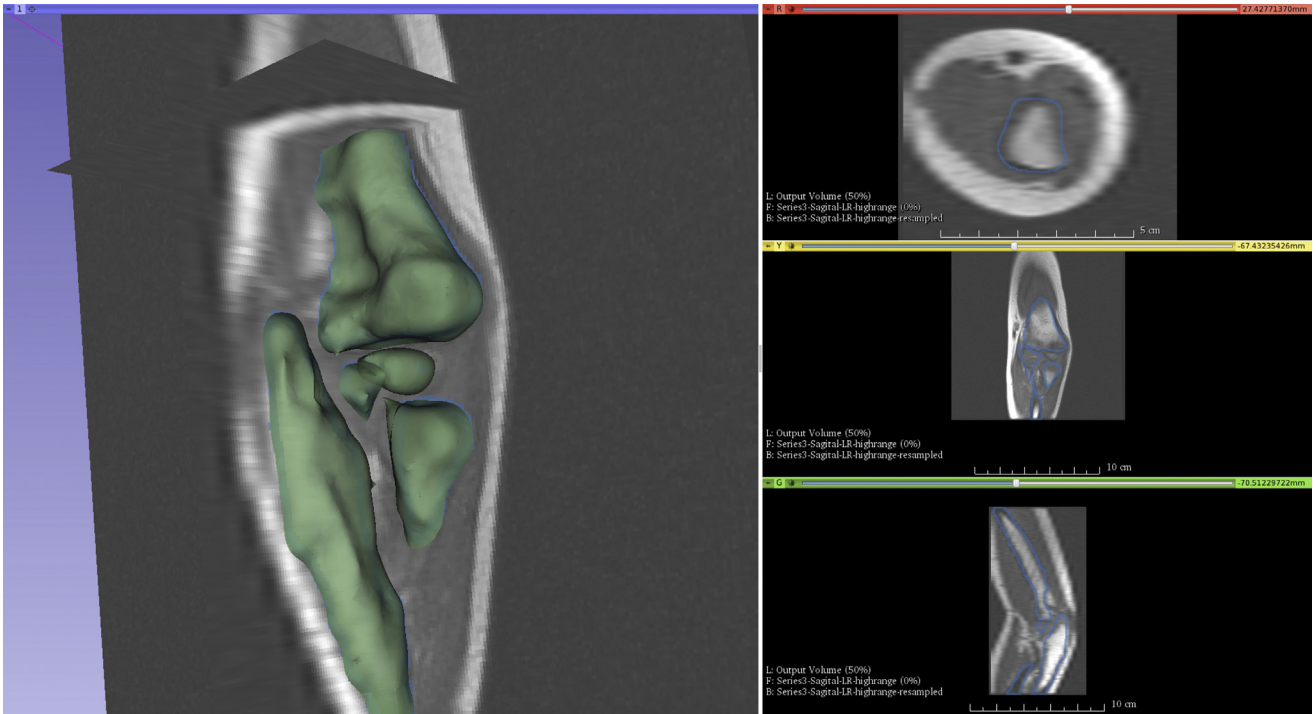


**Figure 3** Segmentation of the magnetic resonance images.

Under general anesthesia, range-of-motion examination was performed using a goniometer. The carrying angle for the right upper extremity was 18° of varus compared to 5° of valgus on the left. Right elbow flexion was 130° compared to 150° on the left. Both right and left elbow had approximately 20° of hyperextension. The right shoulder lacked 20° of external rotation compared to the

left. The surgical procedure was performed with the patient positioned supine with the right upper extremity supported on a hand table. The right upper extremity was prepped and draped, and C-arm fluoroscopy was used to remeasure the humeral-elbow-wrist angle. Two lateral-entry Kirschner (K)-wires were placed through the skin into the capitellum and advanced into the distal humerus. Articular alignment was confirmed with arthrography. The right upper extremity was exsanguinated with an Esmarch bandage, which was then left in place as a tourniquet. The Esmarch bandage was used because of the small size of the patient's arm as the smallest pneumatic tourniquet available at our institution would have partially covered the desired incision and surgical site. The tourniquet was removed after 98 minutes. Hemostasis was maintained and perfusion was confirmed.

The distal humerus was exposed subperiosteally through the interval between the brachioradialis and triceps. A K-wire was

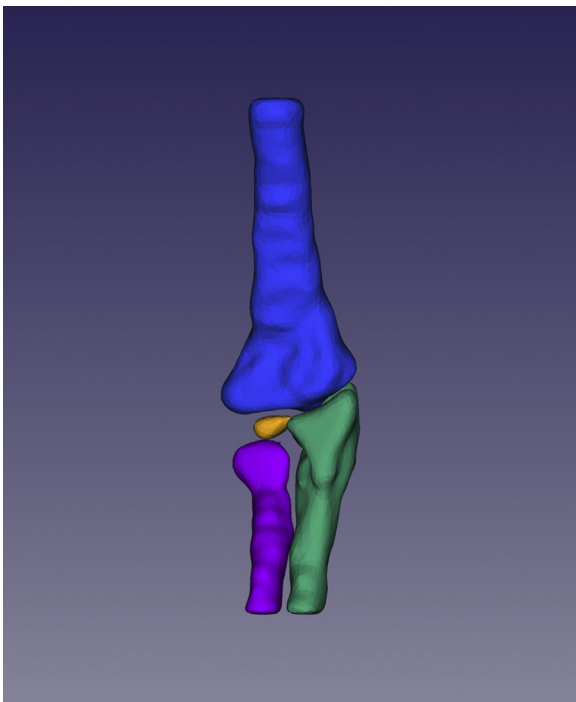


**Figure 4** Computer model produced from segmentation of the magnetic resonance image to create a 3D surface representation of the patient's elbow.

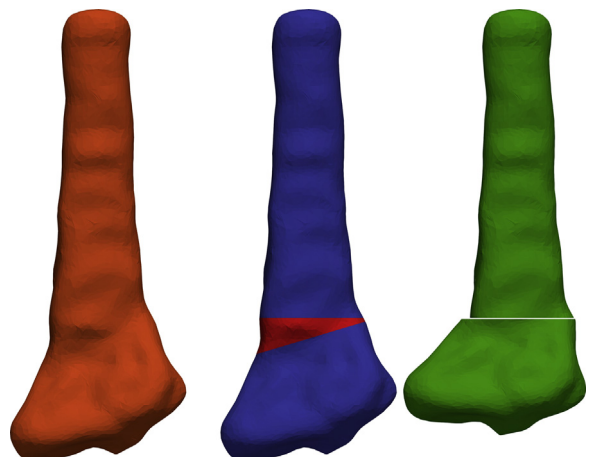


**Figure 5** Virtual corrective osteotomy planned using computer model.



**Figure 6** 3D-printed model with planned cut from the computer model executed in the lab.

inserted parallel to the joint line as confirmed by arthrogram and preoperative planning to use as a reference. The osteotomy was started perpendicular to the shaft of the humerus on lateral view and parallel to the articular surface on anteroposterior view. In accordance with preoperative planning using both the computer model and 3D-printed model to create the appropriate-sized wedge for the desired coronal angular correction, 6 mm was measured proximally along the lateral cortex and a second K-wire was placed to confirm the trajectory, with the planned cuts converging at the medial cortex. Fluoroscopy was used to confirm the desired trajectory and angulation in multiple planes. A saw was used to begin the osteotomy, and the wedge of bone was removed using an osteotome. The planning K-wires were removed and the osteotomy was closed with a slight amount of external rotation to match that planned with the use of the 3D-printed model preoperatively. With the osteotomy reduced, the previously placed distal capitellar K-wires were advanced across into the proximal humerus to provide fixation of the osteotomy. Alignment was confirmed with C-arm fluoroscopy, and the angle between the joint line and the diaphysis was found to be approximately 90°. The range of motion of rotation of the shoulder now matched the contralateral side, confirming the amount of external rotation chosen was appropriate. A final percutaneous lateral entry K-wire was placed for additional fixation and the incision was closed appropriately. The patient was placed in a long arm cast in approximately 70° of elbow flexion. He did well postoperatively and was discharged home the next day. Radiographs taken 4 weeks postoperatively are shown in [Figure 7](#). Casting was discontinued 6 weeks following surgery. At 15 months postsurgery, the patient had improved clinical alignment ([Fig. 8](#)) and range of motion equal to the contralateral side. Radiographs demonstrated neutral alignment of the right elbow with normal-appearing physes. At 28 months postsurgery, the patient continued to have symmetric range of

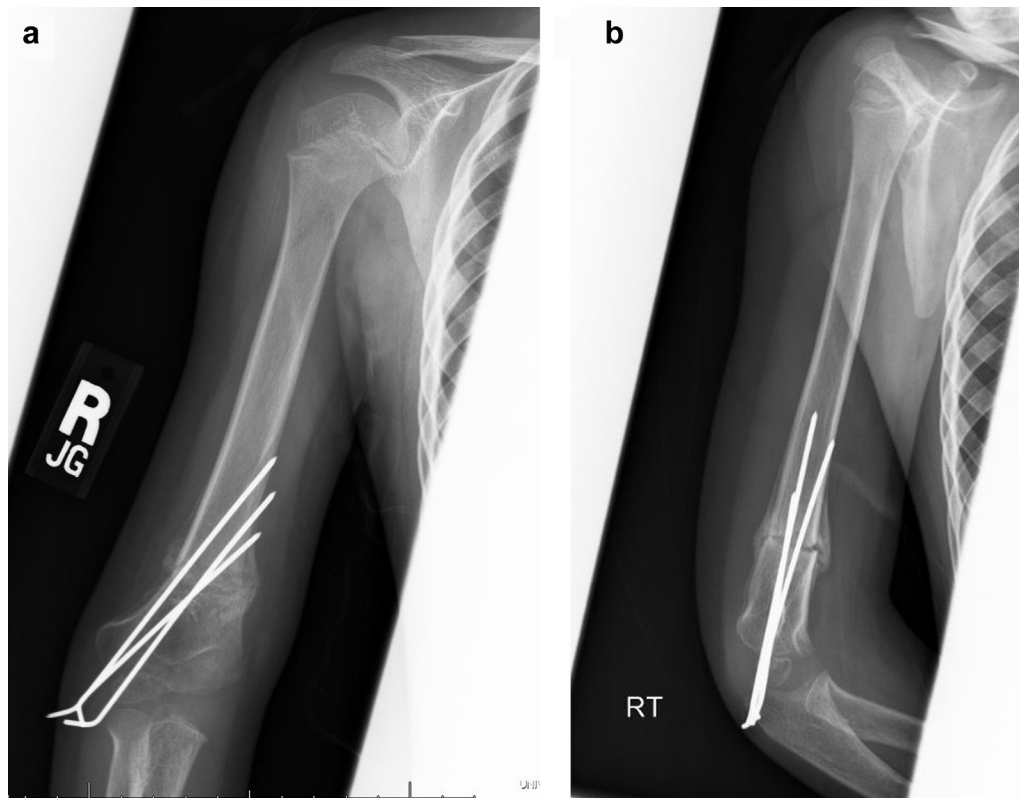


**Figure 7** Anteroposterior (a) and lateral (b) radiographs of the right humerus 4 weeks after surgery demonstrating healing osteotomy with pin fixation in place. The pins were removed without complication at this follow-up visit in the office.



**Figure 8** Clinical photograph taken 15 months postoperatively demonstrating improvement in right upper extremity carrying angle.

motion in both upper extremities and normal neurovascular examination. Radiographs confirmed appropriate alignment and healing (Fig. 9). He was participating in all activities as desired and denied pain.

### Discussion

Supracondylar osteotomies are common procedures for the correction of posttraumatic cubitus varus in pediatric patients.<sup>16,19</sup>

Multiple surgical techniques are described in the literature, and it is difficult to determine if one technique is verifiably superior to the others.<sup>1,4,7,12,14,16,19,22</sup> Regardless, almost all stress the importance of detailed preoperative planning as complications are common and patient satisfaction with cosmetic outcomes remains a concern.<sup>2,3,15</sup>

3D-printed models are a valid way to conduct comprehensive and accurate preoperative planning, especially when performing corrective osteotomy for complex multiplanar deformity.<sup>17</sup> This allows simulation to fine-tune the osteotomy and demonstrates quantitative measurements and anatomic landmarks matching that of the patient's native anatomy to assist in performing the surgical procedure.<sup>5</sup> The impact of this planning method varies. Even when the resulting surgical technique is similar, the location of incisions and the design of the osteotomy are refined to reflect decisions made during practice on the models. Overall, 3D-printed models allow for reduced operating room time and improved clinical outcomes in a majority of patients, with a downside often being increased costs.<sup>8,17</sup> The authors found practicing the correction on the 3D-printed model to be especially useful in planning the rotational portion of the correction, as noting the offset created at the desired rotation of the osteotomy provided another way of confirming appropriate alignment during the procedure.

The potential benefits of in-depth preoperative planning with hands-on practice on a 3D-printed model may be especially seen in surgery for pediatric patients.<sup>5</sup> Surgery becomes more specific and focused, creating a functionally and cosmetically appealing osteotomy while lowering the risk of repeat osteotomy in patients who have such little bone. Accuracy in surgical management is paramount in pediatric patients, as every surgery has long-term implications for the overall health and satisfaction of the child and complications may be devastating.

Relatively little literature is available concerning the use of 3D-printed models for the correction of cubitus varus in children. Multiple examples can be found utilizing 3D-modeling software and 3D-printed surgical guides for preoperative planning and intraoperative assistance, but few go so far as to practice the surgical plan on an anatomically correct model.<sup>13,20,21,23,24</sup> In those

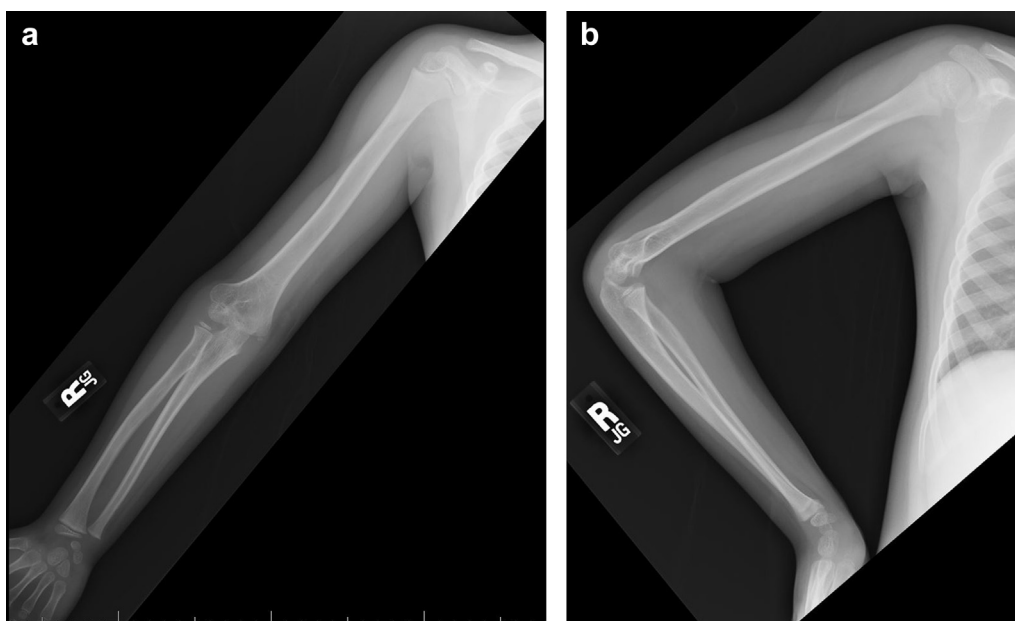


**Figure 9** Anteroposterior (a) and lateral (b) radiographs of the right upper extremity 28 months following surgery demonstrating deformity correction and healing of the osteotomy with preserved physes. There has been appropriate interval growth and appearance of additional ossification centers at the radial head and medial epicondyle.

examples where 3D-printed modeling is used extensively, the patients in question are usually adults.<sup>6,8</sup> In addition, computed tomography is often used to create the 3D model.<sup>8,13,17,20,23,24</sup> However, this results in incomplete visualization of the cartilage portions of the epiphysis in a young child. Because the alignment of the articular surface is critical in achieving a good result, MRI was utilized in this case to build a model including the cartilaginous areas of the distal humerus. MRI has the added benefit of limiting radiation exposure, increasing its utility in pediatric cases.

## Conclusion

The use of 3D printing has been a recent improvement in medicine and has multiple applications. Indications for its use are evolving rapidly. 3D-printed models are a valid way to conduct comprehensive and accurate preoperative planning, especially when performing corrective osteotomy for complex multiplanar deformity. It allows quantitative measurements and anatomic landmarks matching that of the patient's native anatomy to assist in surgical procedure. Further studies will be needed to determine the utility of this new tool in correcting orthopedic deformities in the pediatric population.

## Acknowledgment

The authors would like to thank and acknowledge Laura Bauler, PhD, for her assistance and expertise in editing this manuscript.

## Disclaimer

The authors, their immediate families, and any research foundations with which they are affiliated have not received any financial payments or other benefits from any commercial entity related to the subject of this article.

## References

- Bali K, Sudesh P, Krishnan V, Sharma A, Manoharan SR, Mootha AK. Modified step-cut osteotomy for post-traumatic cubitus varus: our experience with 14 children. *Orthop Traumatol Surg Res* 2011;97:741–9. <https://doi.org/10.1016/j.otsr.2011.05.010>.
- Barrett IR, Bellemore MC, Kwon YM. Cosmetic results of supracondylar osteotomy for correction of cubitus varus. *J Pediatr Orthop* 1998;18:445–7.
- Cho C-H, Song KS, Min BW, Bae KC, Lee K-J. Long-term results of remodeling of lateral condylar prominence after lateral closed-wedge osteotomy for cubitus varus. *J Shoulder Elbow Surg* 2009;18:478–83. <https://doi.org/10.1016/j.jse.2009.02.007>.
- Devnani AS. Lateral closing wedge supracondylar osteotomy of humerus for post-traumatic cubitus varus in children. *Injury* 1997;28:643–7.
- Docquier P-L, Paul L, TranDuy K. Surgical navigation in paediatric orthopaedics. *EFORT Open Rev* 2016;1:152–9. <https://doi.org/10.1302/2058-5241.1.000009>.
- Gemalmaz HC, Sarıyılmaz K, Ozkunt O, Sungur M, Kaya İ, Dikici F. A new osteotomy for the prevention of prominent lateral condyle after cubitus varus correctional surgery—made possible by a 3D printed patient specific osteotomy guide: A case report. *Int J Surg Case Rep* 2017;41:438–42. <https://doi.org/10.1016/j.ijscr.2017.10.048>.
- Hahn SB, Choi YR, Kang HJ. Corrective dome osteotomy for cubitus varus and valgus in adults. *J Shoulder Elbow Surg* 2009;18:38–43. <https://doi.org/10.1016/j.jse.2008.07.013>.
- Inge S, Brouwers L, van der Heijden F, Bemelman M. 3D printing for corrective osteotomy of malunited distal radius fractures: a low-cost workflow. *BMJ Case Rep* 2018;2018. <https://doi.org/10.1136/bcr-2017-223996>.
- Kawanishi Y, Miyake J, Kataoka T, Omori S, Sugamoto K, Yoshikawa H, et al. Does cubitus varus cause morphologic and alignment changes in the elbow joint? *J Shoulder Elbow Surg* 2013;22:915–23. <https://doi.org/10.1016/j.jse.2013.01.024>.
- Lee SC, Shim JS, Sul EJ, Seo SW. Remodeling after lateral closing-wedge osteotomy in children with cubitus varus. *Orthopedics* 2012;35:e823–8. <https://doi.org/10.3928/01477447-20120525-19>.
- Lim TK, Koh KH, Lee DK, Park MJ. Corrective osteotomy for cubitus varus in middle-aged patients. *J Shoulder Elbow Surg* 2011;20:866–72. <https://doi.org/10.1016/j.jse.2011.04.003>.
- Moon MS, Kim SS, Kim ST, Lee SR, Lee BJ, Jin JM, et al. Lateral closing wedge osteotomy with or without medialisation of the distal fragment for cubitus varus. *J Orthop Surg (Hong Kong)* 2010;18:220–3. <https://doi.org/10.1177/230949901001800217>.
- Omori S, Murase T, Oka K, Kawanishi Y, Oura K, Tanaka H, et al. Postoperative accuracy analysis of three-dimensional corrective osteotomy for cubitus varus deformity with a custom-made surgical guide based on computer simulation. *J Shoulder Elbow Surg* 2015;24:242–9. <https://doi.org/10.1016/j.jse.2014.08.020>.
- Pankaj A, Dua A, Malhotra R, Bhan S. Dome osteotomy for posttraumatic cubitus varus: a surgical technique to avoid lateral condylar prominence. *J Pediatr Orthop* 2006;26:61–6. <https://doi.org/10.1097/01.bpo.0000189008.62798.70>.
- Rosseels W, Herteleer M, Sermon A, Nijs S, Hoekstra H. Corrective osteotomies using patient-specific 3D-printed guides: a critical appraisal. *Eur J Trauma Emerg Surg* 2019;45:299–307. <https://doi.org/10.1007/s00068-018-0903-1>.
- Solfelt DA, Hill BW, Anderson CP, Cole PA. Supracondylar osteotomy for the treatment of cubitus varus in children: a systematic review. *Bone Joint J* 2014;96-B:691–700. <https://doi.org/10.1302/0301-620X.96B5.32296>.
- Tack P, Victor J, Gemmel P, Annemans L. 3D-printing techniques in a medical setting: a systematic literature review. *Biomed Eng Online* 2016;15:115. <https://doi.org/10.1186/s12938-016-0236-4>.
- Takeyasu Y, Murase T, Miyake J, Oka K, Arimitsu S, Moritomo H, et al. Three-dimensional analysis of cubitus varus deformity after supracondylar fractures of the humerus. *J Shoulder Elbow Surg* 2011;20:440–8. <https://doi.org/10.1016/j.jse.2010.11.020>.
- Tanwar YS, Habib M, Jaiswal A, Singh S, Arya RK, Sinha S. Triple modified French osteotomy: a possible answer to cubitus varus deformity. A technical note. *J Shoulder Elbow Surg* 2014;23:1612–7. <https://doi.org/10.1016/j.jse.2014.06.030>.
- Tricot M, Duy KT, Docquier PL. 3D-corrective osteotomy using surgical guides for posttraumatic distal humeral deformity. *Acta Orthop Belg* 2012;78:538–42.
- Vlachopoulos L, Schweizer A, Meyer DC, Gerber C, Furststahl P. Three-dimensional corrective osteotomies of complex malunited humeral fractures using patient-specific guides. *J Shoulder Elbow Surg* 2016;25:2040–7. <https://doi.org/10.1016/j.jse.2016.04.038>.
- Yang J, He T, Liu S, Peng M, Liu M. Lateral closing wedge osteotomy for treatment of traumatic cubitus varus deformity in children. *Zhongguo Xue Fu Chong Jian Wai Ke Za Zhi* 2012;26:657–60 [in Chinese].
- Zhang YZ, Lu S, Chen B, Zhao JM, Liu R, Pei GX. Application of computer-aided design osteotomy template for treatment of cubitus varus deformity in teenagers: a pilot study. *J Shoulder Elbow Surg* 2011;20:51–6. <https://doi.org/10.1016/j.jse.2010.08.029>.
- Zheng P-F, Chen J, Xux XP, Jiang B, Yao Q-Q, Wang L-M. [Accurate osteotomy assisted by individualized navigation templates for the treatment of children cubitus varus]. *Zhongguo Gu Shang* 2017;30:377–82. <https://doi.org/10.3969/j.issn.1003-0034.2017.04.020>.